

Article

The Effect of Stress Level on the Resilient Modulus of Non-Engineered Mudrock Backfill Materials

Shaymaa Kennedy, Sam Clarke  and Paul Shepley

Department of Civil & Structural Engineering, University of Sheffield, Mappin Street, Sheffield S1 3JD, UK; skkennedy1@sheffield.ac.uk (S.K.); pshepley@gmail.com (P.S.)

* Correspondence: sam.clarke@sheffield.ac.uk; Tel.: +44-(0)114-222-5703

Abstract: In the UK, High Speed Rail 2, (London to the ‘North’) is surrounded by a number of questions regarding construction technologies which can minimise the impact of the route. The rail industry in the UK has vast experience based with ballasted track, but this is not necessarily the most appropriate choice for new high speed rail construction when crossing problematic soils. This paper aims to investigate the use of different track types (ballasted and ballastless) and the influence they will have on the underlying soil in areas predominated by non-engineered mudrock backfills, relics of the UK’s mining heritage. Mudrocks are a class of fine-grained siliciclastic sedimentary rocks. Structural performance of the railway track strongly depends on the level of stress that is transmitted to the ground and this must be reduced to an acceptable level to minimise deterioration in the mudrock if they are to be utilised effectively. The main objective for this paper is to investigate the impact of the initial stress conditions and dynamic stress on the permanent deformation of mudrock under different physical conditions. Triaxial testing is used to estimate the stiffness characteristics of the mudrock. The results show that the resilient modulus increases with a decrease in the stress amplitude. In addition, ballasted track shows a higher suitability for use in design in terms of the stiffness generated within the mudrock.



Citation: Kennedy, S.; Clarke, S.; Shepley, P. The Effect of Stress Level on the Resilient Modulus of Non-Engineered Mudrock Backfill Materials. *CivilEng* **2022**, *3*, 630–642. <https://doi.org/10.3390/civileng3030037>

Academic Editor: Aires Camões

Received: 3 March 2022

Accepted: 14 July 2022

Published: 20 July 2022

Publisher’s Note: MDPI stays neutral with regard to jurisdictional claims in published maps and institutional affiliations.



Copyright: © 2022 by the authors. Licensee MDPI, Basel, Switzerland. This article is an open access article distributed under the terms and conditions of the Creative Commons Attribution (CC BY) license (<https://creativecommons.org/licenses/by/4.0/>).

Keywords: mudrocks; resilient modulus; dynamic loading

1. Introduction

Railway infrastructure consists of a track superstructure (namely rails and associated components) and substructure which support these rails (ballast, sub-ballast, and sub-grade), as shown in Figure 1a,b. Much research has gone into minimising the wear on the rail–wheel interface [1,2]. This wear is also known to be a product of the quality of the track substructure. This supporting structure needs to be durable to minimise ongoing maintenance and to optimise the use of materials such as concrete and ballast from an environmental perspective. The performance of the overall track design also depends on the behaviour of the ground (natural or remediated) over which the railway is constructed.

In the UK there exist large expanses of non-engineered backfills, specifically a historic product of the coal mining industry. Many of the coal-rich layers are interspersed with mudrocks [3], leading to the creation of areas of non-engineered backfill where the mudrock spoil is placed. The initial inundation collapse [4,5] and subsequent behaviour [6] of these fills is well-documented, but what remains unknown is their response to cyclic loading brought about by railway construction over these now-remediated areas.

The dynamic response of the overall track strongly depends on the properties of individual elements of the track structure and the interaction between train movement and underlying soil [7]. With all laboratory testing, the stress conditions recreated should represent the physical conditions present in the problem to be investigated. For track subgrades this is a combination of the vertical stresses applied by the substructure above the point of interest and the dynamic stresses induced by railway traffic. Kempfert et al. [8]

reported that the in situ dynamic stresses induced by railway traffic were dependant on train speed, type of substructure, depth, and soil type, as shown in Figure 1d. Dynamic stress levels were reported to be the highest in ballasted track, reaching a peak of ≈ 50 kPa, 0.86 m from the surface directly under the rail location, to a minimum of 5 kPa at a depth of 1.48 m below. It was also found there was an attenuation of the induced dynamic stresses with increasing depth. Bian et al. [9] found that the impact of dynamic stress on depth extends much deeper in ballasted tracks and that the stresses range between 50–100 kPa, whilst in the ballastless tracks this is reduced to 13–20 kPa. A comparison of the stress conditions experienced by the subgrade is shown schematically in Figure 1. Bian et al. also found that whilst the train speed had an effect on the stresses generated, this was a second order effect when compared with the attenuation with depth.

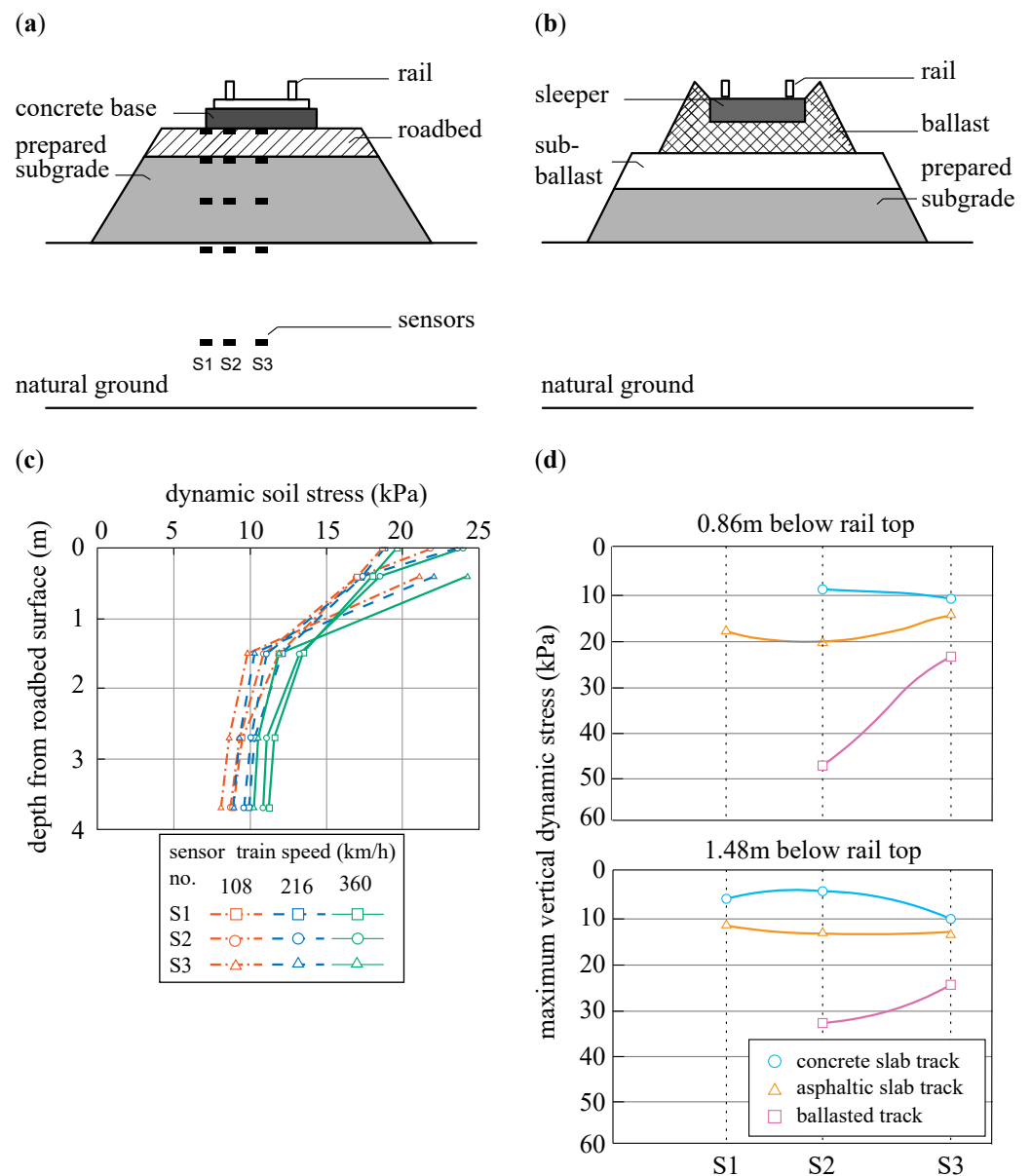


Figure 1. Schematic diagram of (a) typical ballastless track, (b) typical ballasted track, (c) dynamic stress distributions with depth under ballastless track adapted with permission from Ref. [9]. 1999, Elsevier, (d) comparison of ballasted and ballastless track stress distributions, adapted from Ref. [8].

To find an adequate design against long-term track deterioration, the response of the soil under repeated loading must be quantified. The resistance of a track subsoil to cyclic

loading can be characterised by measuring the resilient modulus for a given stress state. To assess the performance of a subgrade, the cyclic triaxial test is used to estimate the stiffness (resilient modulus) and strength characteristics of the soil.

For design purposes, it is important to consider how the materials involved in the design react and how the resilient behaviour varies with changes in various influencing factors. Fredlund et al. [10] proposed a theory between resilient modulus and stress conditions for cohesive subgrade soils and established the relationship between resilient modulus and stress state for specimens subjected to 100 stress cycles. Resilient modulus was found to be affected by an increase in deviator stress and matrix suction. Whilst numerical models also exist to predict the long-term cyclic deterioration of railway tracks [11], physical test data is always required to inform the models.

The dynamic load that is induced from the movement of the train can be considered according to a theoretical analysis of a stress wave penetration into the soil. This load, applied from the passage of the wheels, generates stress pulses in the soil. Each pulse includes three components: vertical, horizontal, and shear, causing rotation of the principal stress axes [12]. This has led researchers to use the hollow cylinder apparatus to investigate this [13].

At the start of a test, particle rotation and rearrangement produce the plastic strain. Thus, with an increase in the number of cycles, the particle movements become limited and continued strain reduces due to the increased particle contacts. Previous studies have indicated that a large number of cycles is not required for certain soil types [14]. However, there is no pre-defined number of cycles required for this stabilization to occur. Stewart [15] achieved stabilization after 1000 cycles for a typical ballast material, while Lackenby [16] indicated that stabilization occurred at 100 cycles for granular materials. Suiker et al. [17] tested granular soils with up to 5 million cycles with stability occurring after 1000, supporting the work of Stewart. However, for these granular materials, the durability of the individual particles is high, unlike that of mudrock [18]. Thus, the number of cycles required for stabilisation depends on material type, water content, and stress level and will be investigated for mudrocks in the current study.

This paper presents the results of two studies. The first is a study on the behaviour of track type (ballasted or ballastless) induced states on the resilient modulus. The second study is an extension of this to include higher stress states in an attempt to generalise the results.

2. Materials and Methods

The material of study, mudrock colliery spoil, was collected on 10 August 2015 from Kellingley Colliery, North Yorkshire, England. This was stored in a covered crate outside the research laboratory at the University of Sheffield from collection. This material can be described as a weathered dark grey mudrock and has a variety of particle sizes to a maximum of 30 mm. According to the triaxial cyclic load testing protocol given in [19], the maximum particle size allowed in a test is 1/6 of the diameter of the triaxial cell to be utilised. In the current testing, a 100 mm diameter cell was used, which gives a maximum particle size of 16 mm. Particles bigger than 10 mm were removed due to their angular shape, which led to difficulties when compacting specimens. The effect of compaction was also investigated in the current study to enable the influence of degradation on performance to be quantified. Thus, samples produced with only <5 mm particles were chosen to shed light on the effect of degradation on the cyclic performance. Particle size distribution tests were undertaken, showing that the spoil could be classified as poorly-graded for the <10 mm and <5 mm samples for the results shown in Figure 2. The values of D_{10} , D_{30} , and D_{60} are 4.6, 8.0, and 10.4 mm, respectively, for the as-received material. The specific gravity, G_s , was found to be 2.75. The coefficient of uniformity ($C_u = D_{60}/D_{10}$) and the coefficient of curvature ($C_c = (D_{30})^2/(D_{60} \times D_{10})$) are given in Table 1 after an indicative cyclic test, due to the continued particle degradation. Figure 2 displays the effect of compaction and cycling on the degradation of the mudrock. The mudrock was sieved to prepare for

compaction and then compacted to be ready for the test. Specimens were dried in the oven after compaction and sieved again. It can be seen that the change of particle size distribution after compaction was 56% at D_{30} . It can be seen that there is a change of particle size distribution after compaction, compared with only a minor further reduction in size.

The permeability, k , calculated for this material is based on the empirical relationship given by [20]:

$$k = 1.99 \times 10^4 \left(\frac{100\%}{\sum [f_i / (D_{li}^{0.404} \times D_{si}^{0.595})]} \right)^2 (1/SF^2) \times [e^3 / (1 + e)] \quad (1)$$

where SF is the shape factor (ranging from 6.0 for spherical to 8.4 for angular) and e is the void ratio. For i sieve pairs used, D_{li} is the larger size and D_{si} is the smaller, with f_i being the fraction of particles between two sieve sizes. Following Equation (1), the permeability for the compacted particles passing through a 10 mm sieve was 0.0337 m/s and for particles passing through a 5 mm sieve was 0.0203 m/s. Hence, the soil was classified as being semi-pervious or having a moderate permeability [21].

Table 1. Particle size distribution classification.

Particle Size	D_{10}	D_{30}	D_{60}	C_u	C_c
<10 mm	2.25	4.4	7	3.1	1.22
<5 mm	0.5	1.5	3.2	6.4	1.40

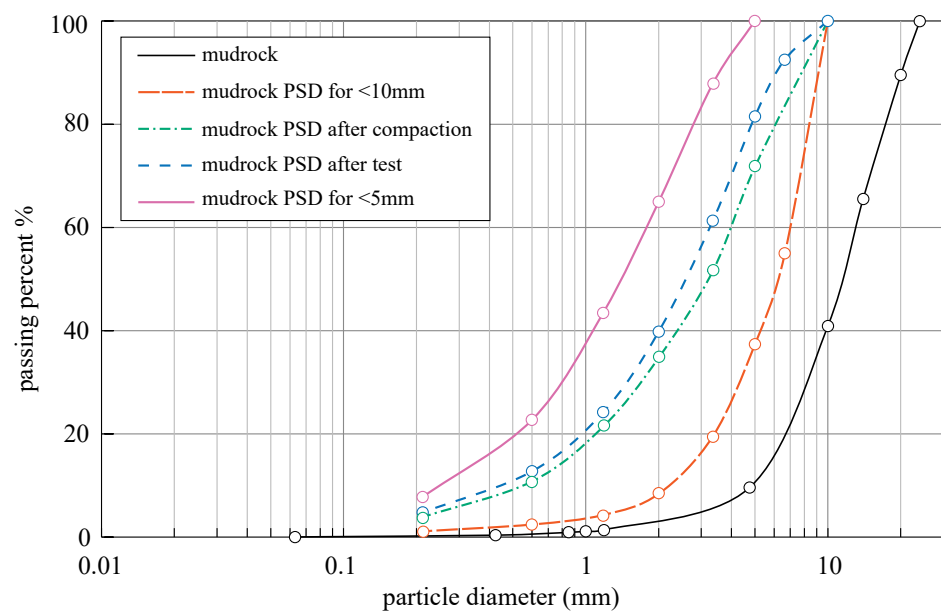


Figure 2. Particle size distribution and the effect of compaction and cyclic on the degradation of materials of study.

To assess the durability of the larger particles, slaking tests were performed [22]. The results classify the mudrock as having medium slake durability. Figure 3 shows the degradation of the soaked particles with repeated slaking cycles.



Figure 3. The effect of slaking on mudrock (a) before slaking, (b) after first cycle, (c) after second cycle.

All tested specimens were compacted according to the information given in Table 2. Each saturated specimen was saturated prior to testing, representing the worst case scenario that could occur due to fluctuations in the groundwater table. In the saturated condition, the B-value was 0.95–0.96, guaranteeing the specimens were close to full saturation. The specimens were tested under two conditions: partially saturated and saturated cases. In the UK, High Speed Rail 1 (HS1) trains run at speeds between 230 km/h (143 mph) to 300 km/h (186 mph) with a train length of 108 m. In this study, load frequencies of 4 Hz and 1 Hz were used for testing and are indicative of the frequencies induced by HS1.

Table 2. Compaction properties for mudrock.

Test Compaction	PSD	Dry Density, mg/m ³	Water Content %	Saturation %	Void Ratio
At maximum dry density		2.04	11	88	0.34
At dry side	<10	1.98	10.5	75	0.38
At maximum dry density		2.11	8.5	77	0.30
At dry side	<5	2.05	7.8	65	0.33

The triaxial testing system was manufactured by ELE International, UK, and Industrial Process Controls Ltd. The system consists of a triaxial cell, a load frame and a Control and Data Acquisition System (CDAS) from UTM, linked to a computer. The triaxial cell can test specimens of up to 200 mm high and 100 mm in diameter with a suction top cap allowing a constant connection to the sample top. The cyclic triaxial system is shown in Figure 4. Details of the triaxial cyclic load control software can also be found in [23]. Stresses were applied for each sample as shown in Table 3, based on [8,9].

Table 3. Test programme overview.

Depth (m)	σ_c	σ_v	σ_{cyclic}^*	σ_{cyclic}^{**}	q	p'	SR *	SR **
1	18	20	40	20	2	18.7	2.14	1.07
2	27	40	30	10	13	32.0	0.93	0.31
3	40	60	20		20	46.7	0.43	
4	55	80	10		25	63.3	0.16	

Notes: * = ballasted, ** = ballastless, SR = stress ratio. All stress in (kN/m²).

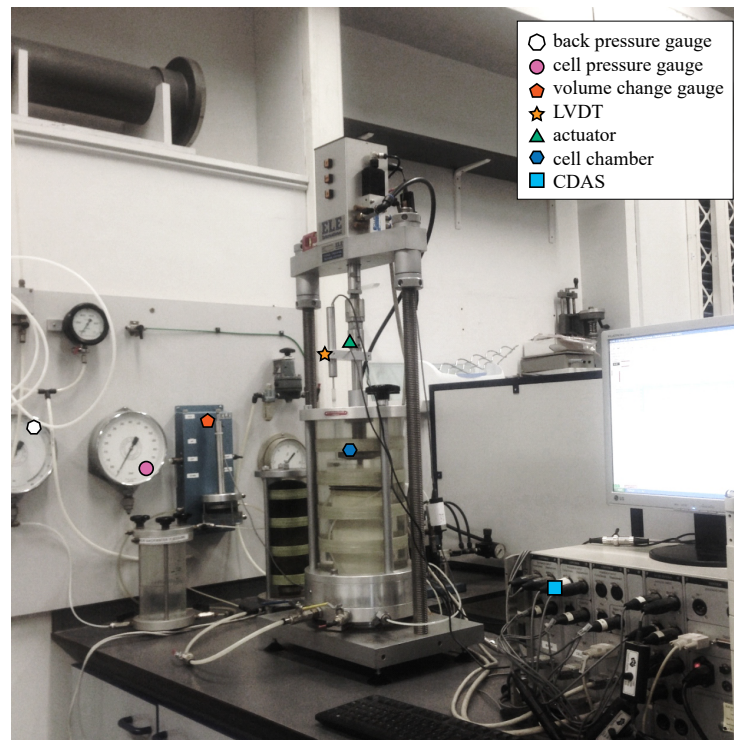


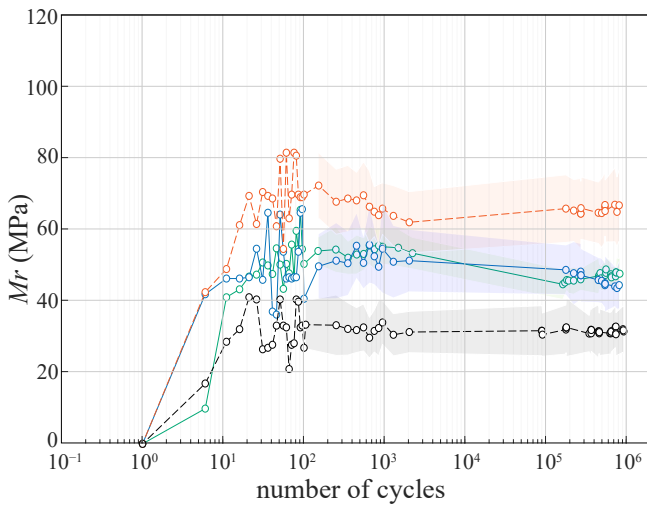
Figure 4. Triaxial cyclic apparatus.

3. Experimental Issues

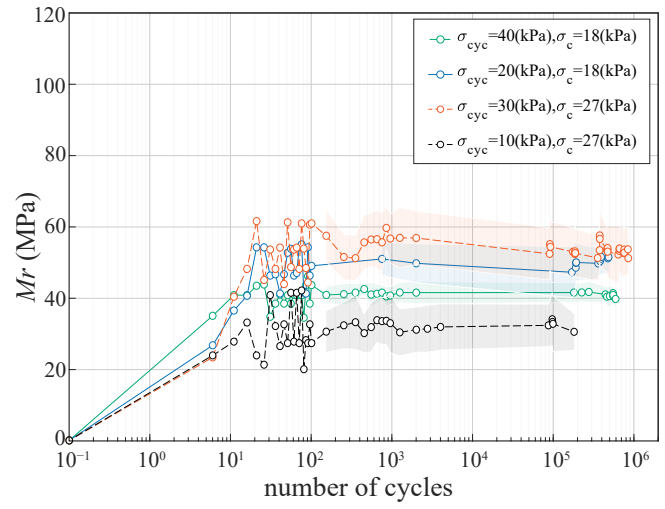
In the UTM apparatus control software, loading is applied continuously until either the termination strain level is exceeded or it is stopped manually by the operator. To apply a compressive sinusoidal load, the loading pulse wave shape was set in the UTM software to be haversine. The storage of information in the UTM software depends on the loading rate and loading sequence. For a test consisting of 10^6 cycles, the software only stores 626 data points. This is hard-programmed into the software and is not user configurable. The software was originally designed for slow cycles taking many seconds, not for thousands of cycles at high frequency [24]. To collect as much data as possible, 10^5 cycles were applied for two different frequencies.

In the 1 Hz tests, the first 500 cycles were captured, each being represented by a single data point. The data are then not stored until 64,128 cycles, at which time each data point from cycle 64,128 to 10^5 represents an average of 128 cycles. Testing at 4 Hz, each data point represents the average of 5 cycles, which is maintained for the first 2496 cycles. The data is then not stored until 80,156 cycles, at which time each data point from 80,156 to 10^5 cycles each data point represents the average response over 160 cycles. The resilient modulus was calculated from the average data in each case, with the results being shown in Figure 5.

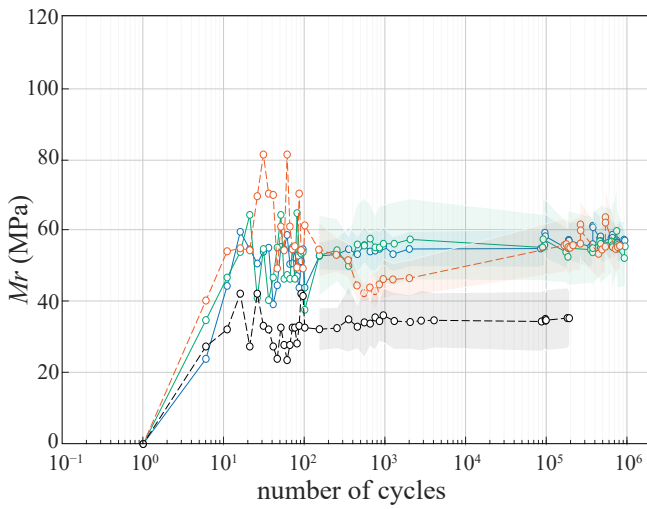
In Figure 5a–d, the first hundred data points are plotted raw. From 106 to 2496 cycles the data points represent the average resilient modulus, with the standard deviation shown as the shaded area. The same is true for the data points between 80,156 and 10^5 cycles data where the average with standard deviation was again plotted. In Figure 5e,f, the first hundred data points are again plotted raw with the remaining data points representing the average resilient modulus for 1000 cycles. Again, the shaded areas represent the standard deviation.



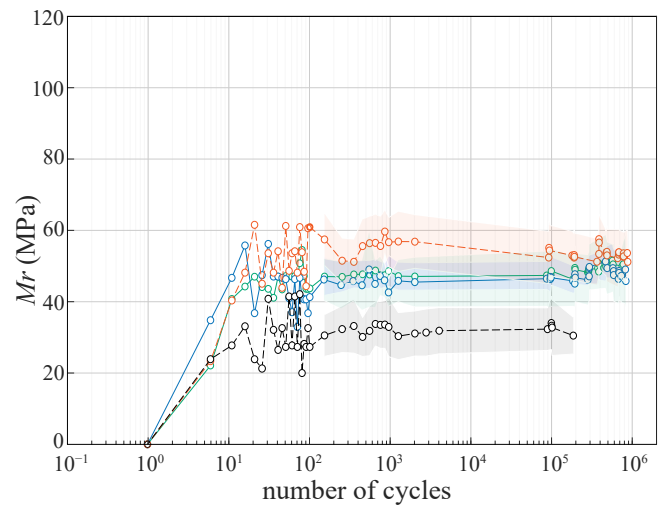
(a) Particles < 10 mm, 4 Hz at OMC



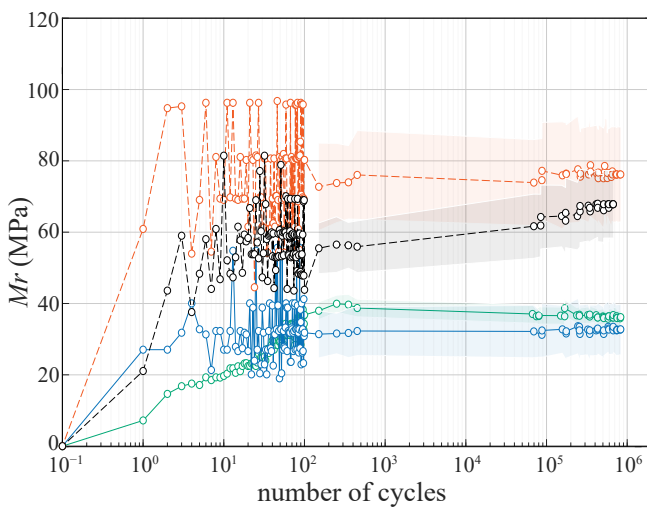
(b) Particles < 5 mm, 4 Hz at OMC



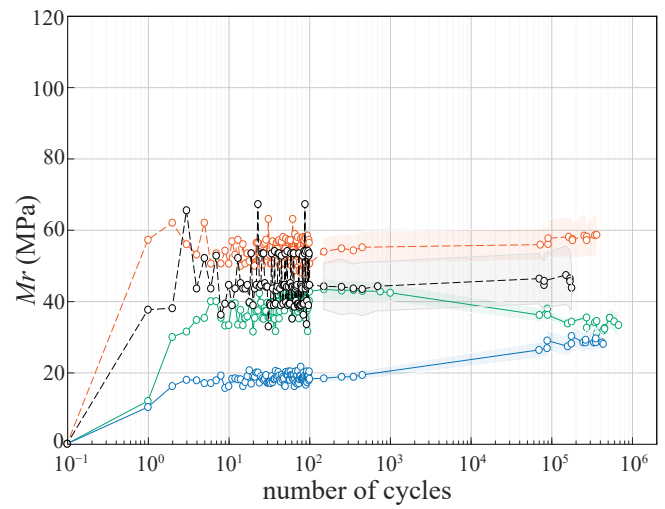
(c) Particles < 10 mm, 4 Hz, saturated



(d) Particles < 5 mm, 4 Hz, saturated



(e) Particles < 10 mm, 1 Hz, saturated



(f) Particles < 5 mm, 1 Hz, saturated

Figure 5. Effect of confining pressure and frequency on the resilient modulus for saturated and OMC states, with shaded areas indicating standard deviation.

4. Results

4.1. The Effect of Track Type Induced Stress States on Resilient Modulus

The stress induced only has an influence on the track subgrade up to a depth of 2 m for ballastless and 4 m for ballasted track construction. At 2 m, the confining pressure, $\sigma_c = 27$ kPa whilst the cyclic loading required to recreate the conditions at 2 m depth is $\sigma_{cyclic} = 30$ kPa for ballasted and $\sigma_{cyclic} = 10$ kPa for ballastless track types (Table 3). Both partially saturated at optimum moisture content and fully saturated conditions have been chosen to evaluate the effects. The purpose of these tests was to define the effect of cyclic loading stress on the soil stiffness. The cyclic frequency was either 4 Hz or 1 Hz. With 4 stress conditions, 2 frequencies, 2 particle size distributions, and 2 compaction conditions, the matrix of all possible test combinations is impossibly large, especially considering the duration of each test (1–2 weeks). The testing conducted is designed to allow the interaction between these test conditions to be inferred rather than directly tested. An example of this would be that no testing was done at OMC at 1 Hz, as there was no pronounced effect caused by the frequency change for saturated samples.

Figure 5 shows the results from 24 individual specimens. Specimens were tested in both saturated and optimum moisture content (OMC) conditions for two different particles distributions and load frequencies. The resilient modulus has been plotted against number of cycles to determine their effect in turn. The results are categorised according to the soils conditions used to simplify the interpretation of results.

Figure 5a shows that, in broad terms, increases in both cyclic stress and confining pressure lead to an increase in the resilient modulus. The specimen tested under $\sigma_{cyclic} = 30$ kPa exhibited an initial stiffening over the first ≈ 100 cycles and the highest overall M_r of 68 MPa. The specimen with a cyclic stress of $\sigma_{cyclic} = 10$ kPa showed the lowest increase in modulus to just 36 MPa. There was a fluctuation of the resilient modulus in all specimens between 200 and 10^4 cycles, likely due to the breakage of particles, after which the soil behaved more stably between 10^5 – 10^6 cycles.

Similarly, Figure 5b reveals that the performance of specimens with particles < 5 mm behaved in the same manner, with a general tendency to be less stiff compared to the specimens with larger particles. It can be also seen that for the specimens tested at $\sigma_{cyclic} = 30$ kPa and $\sigma_{cyclic} = 10$ kPa equilibrium is reached at the same point $\approx 10^3$ cycles, leading to a modulus of 53 MPa and 30 MPa, respectively, at 10^6 cycles.

Figure 5c attempts to isolate the effects of moving from OMC conditions (Figure 5a) to saturated. Interestingly, for 3 of the 4 specimens, the resilient modulus reached appears to be independent of cyclic stress and confining pressure applied; a plateau of 55 MPa. The $\sigma_{cyclic} = 30$ kPa specimen showed an uncharacteristic reduction in modulus in the 300–400 cycle region, possibly due to a void collapsing within the specimen. This then returns to the expected levels at $\approx 10^5$ cycles. For the specimen with $\sigma_{cyclic} = 10$ kPa, an initial stiffening over the first ≈ 100 cycles led to a resilient modulus of 32 MPa.

Figure 5d investigates the same move to saturated conditions, but for specimens with particles < 5 mm. A similar trend is seen as in Figure 5c, albeit with a slightly reduced modulus being reached (50 MPa) compared to the specimens tested under OMC conditions. For all of the $\sigma_{cyclic} = 10$ kPa specimens tested at 4 Hz, the resilient modulus remains unchanged.

The resilient modulus for mudrock under 1 Hz loading was also examined to assess whether the stress states shown in Figures 5a–d would be affected by frequency (albeit, only for saturated specimens). The results shown in Figure 5e show that for specimens with < 10 mm particles there is an increase in resilient modulus for $\sigma_{cyclic} = 10$ and 30 kPa specimens for a decrease in cyclic frequency. The results indicate that for 1 Hz testing the confining stress governs the response, with the two specimens with a $\sigma_c = 18$ kPa showing a 50% reduction over the specimens tested with a $\sigma_c = 27$ kPa.

Figure 5f plots the resilient modulus for specimens tested at 1 Hz with < 5 mm particles. This shows no major change in the maximum modulus when compared with results from the 4 Hz tests. The same $\approx 50\%$ reduction is still apparent in the specimens tested at $\sigma_c = 18$ kPa, as was seen in Figure 5e.

Regarding the number of cycles required, generally all tests in Figure 5 reach an early equilibrium within the first 1000 cycles, with no notable increases with further cycles. This is a valuable finding for future research into the cyclic response of friable materials such as mudrock.

4.2. Effect of Cyclic Loading and Confining Pressure on Resilient Modulus

To further assess the impact of stress state on the resilient modulus, variable stress distributions were applied to specimens tested under optimum moisture content and fully saturated states at 4 Hz.

Results shown in Figure 6 demonstrate the varying effect increasing the confining pressure with a decrease in the magnitude of cyclic loading has. Common trends are hard to discern from the results. One common result was for the highest $q_{max} = 90$ kPa specimens, which exhibited the lowest resilient modulus consistently through all conditions. The results also indicate that a decrease in particle size leads to slightly lower generated resilient moduli in most specimens. As with Figure 5, equilibrium in the specimens is reached within the first 1000 cycles, with this value being maintained up to 10^5 cycles. It can also be seen that small cyclic stresses can still cause degradation of soil, leading to lower resilient modulus, e.g., $q_{max} = 90$ kPa test in Figure 6a. The notable exception in the trends is specimen $q_{max} = 60$ kPa test in Figure 6a, where the modulus decreased after 2000 cycles.

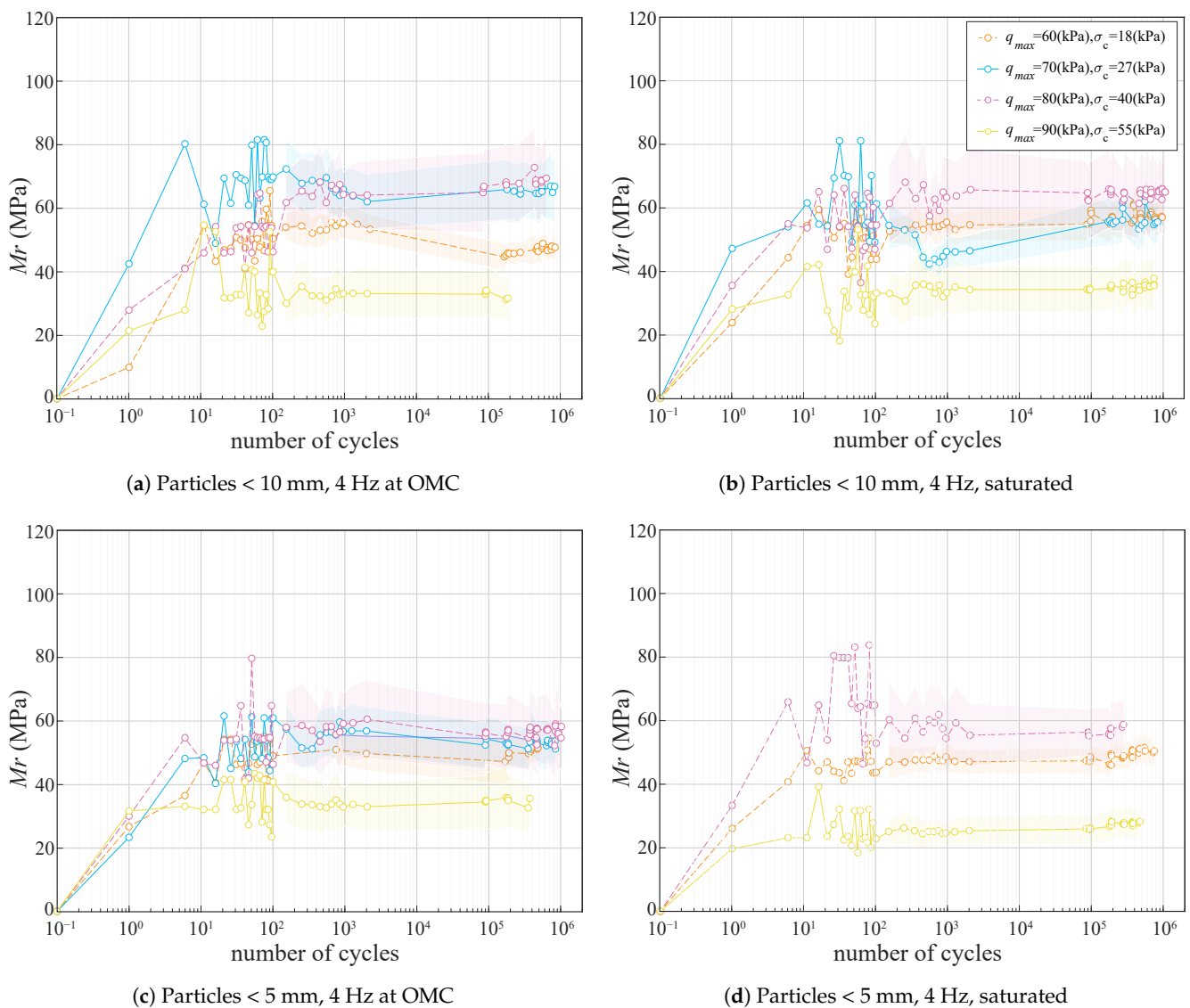


Figure 6. Effect of confining pressure on stiffness for OMC and saturated states, with shaded areas indicating standard deviation.

Figure 6b shows plots for the specimens with particles <5 mm. The same trends in behaviour can be seen as in Figure 6a. Again, the specimens with the lower confining stresses (and hence higher stress ratios) display similar moduli ≈ 60 MPa, which repeats the trends seen in Figure 5c.

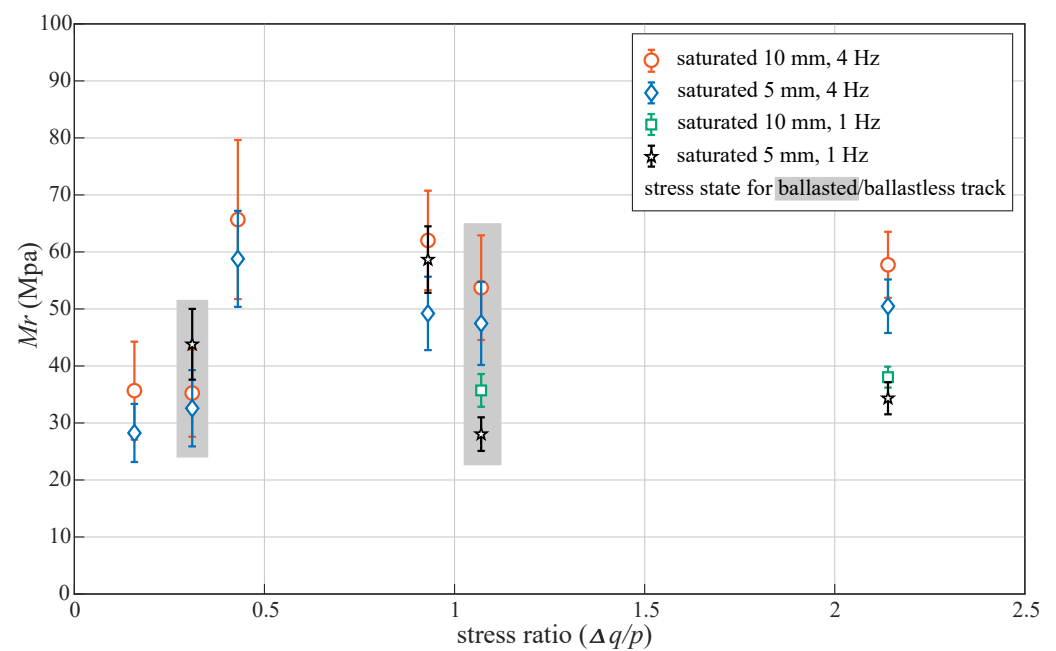
In saturated conditions, the specimens behave similarly to those tested under partially saturated at OMC conditions (Figure 6c), with slightly lower moduli seen in all stress states. As before, the effect of reducing the maximum particle size to 5 mm keeps the same pattern of behaviour but with a marginally lower resilient modulus (Figure 6d). The $q_{max} = 70$ kPa data is missing from Figure 6d due to a failure in the confinement to the specimen, which was only noticed during processing after the test series was complete.

5. Discussion

The current findings show that an increase in cyclic deviatoric stress with a constant confining pressure will act to increase the resilient modulus. To better understand the trends in the data, the resilient modulus for all tests were compared using stress ratio (q/p') and were plotted versus the Mr attained at 5×10^5 cycles in Figure 7a,b. The stress ratio varied from 2.14 to 0.16, according to the conditions simulated (Table 3). With high stress ratios ($q/p' > 1$), the resilient modulus is relatively stable. In this region the particle size affected the attained modulus for 1 Hz and 4 Hz frequencies by reducing the Mr by 4% and 11%, respectively, for a reduction in the maximum particle size from 10 to 5 mm. It can also be seen that the Mr was higher for increased load frequency.

For stress ratios between 0.4 and 1, the performance improved as the attained modulus was higher in all like-for-like tests. The highest stiffness of any test was developed in the 1 Hz under OMC conditions for particles < 10 mm. For stress ratios below 0.4, all the specimens exhibited low resilient modulus.

Generally speaking, the resilient modulus increased with a decrease in stress ratio until reaching $q/p' = 0.31$, at which point the specimens became less stiff for any given moisture content condition. In addition, decreasing stress ratio under the same confining pressure led to a decrease in resilient modulus stress ratio (see results at $q/p' = 1.07$ and 0.31).



(a) Saturated conditions

Figure 7. Cont.

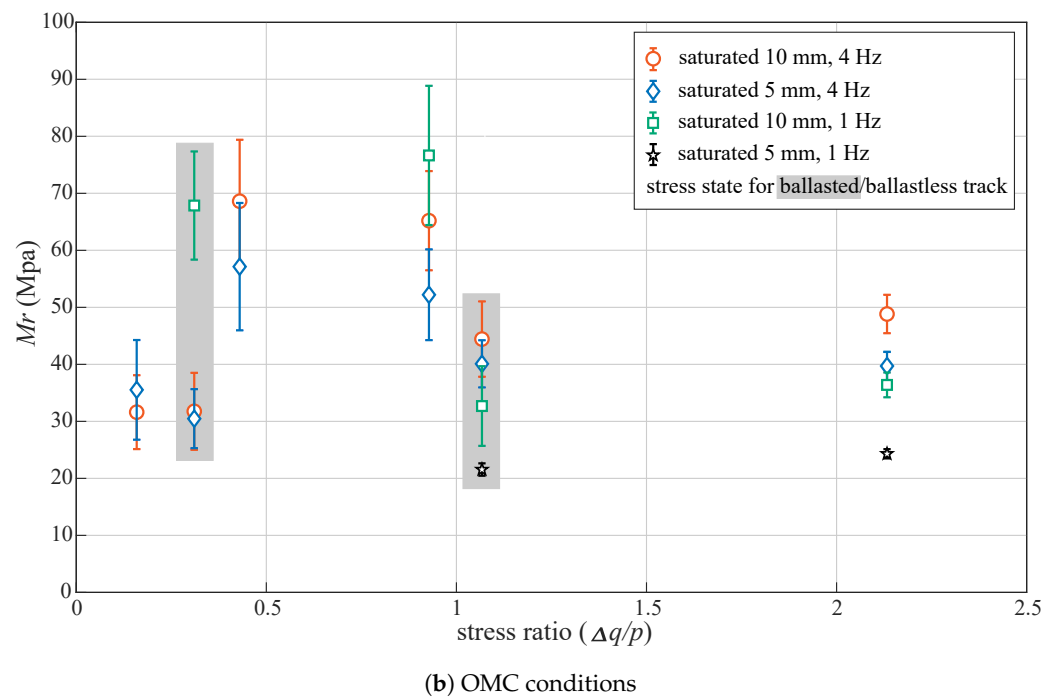


Figure 7. Development of resilient modulus with varying stress ratio.

The value of resilient modulus for mudrock can be classified as a ‘good’ modulus according to the classification for track and subgrade modulus [25]. The results indicate that an increase in cyclic deviatoric stress leads to an increase in stiffness (Mr). Nevertheless, this does not mean a stiffer layer would behave badly due to higher cyclic deviator stress because the performance of soil not only depends on stress state but also on the strength of soil. In the comparison between ballasted and ballastless stress distributions, it was shown that the resilient modulus for ballasted systems was larger than that in ballastless due to the deviator stress being higher. This is due to the increment of strength being much higher than the increase in deviator stress [26].

6. Conclusions

It is well known that the resilient modulus, Mr , can be used to quantify the long-term cyclic performance of soils. In this paper, the resilient modulus has been used to quantify the long-term response of soils under varying distributions of stress.

The stress distributions that were induced below ballasted and ballastless track structures were estimated from the literature and specimens were tested under the same stress states in the laboratory. Cyclic deviator stresses are lower in ballastless track types than in ballasted as the thickness of the first layer is higher, which spreads the loading and reduces the stress.

Results of the slaking test and compaction particle size distribution data showed that breakage led to an increase in fine content after compaction. Hence, soil permeability could also be affected, which could lead to the soil not meeting the design requirements. Filter materials could be used in this case to maintain drainage in the soil. Further research is needed to conduct seepage tests under the same conditions as in the field, to investigate the performance of drains, and therefore guarantee track performance.

Results showed that mudrock subjected to the stress distribution for a ballastless system had a modest decrease in stiffness of around 6% compared to that seen in the ballasted stress state. However, increasing deviatoric stress and confining pressure led to a decrease of the stiffness of the ballastless track to around 54%. In addition, the effect of changing stress distribution on the resilient modulus was highlighted. The results showed that stiffness increases with a decrease in the stress ratio q/p' until the maximum at 0.43

(higher deviatoric stress is reached). The M_r then decays by around 50–55% for stress ratios down to 0.134.

A ballastless track system can be capable of reducing the amount of maintenance required by 10–30% compared to ballasted track. However, the stress conditions generated by ballasted track showed a greater suitability for use in design in terms of the stiffness generated in the subgrade. Ballastless produces less settlement due to the cumulative strain being dependent mainly on the deviatoric stress. This is particularly the case for the smaller particles, as bigger particles are more resistant to breakage and densification with further cycles. This conclusion supports previous work done by [27–29].

To make good use of the results of the cyclic triaxial tests for the possible use of mudrock as a subgrade (or more likely as an existing non-engineered backfill), it is necessary to take into account the traffic weight, maintenance schedule, and allowable values of elastic and plastic deformations of the subgrade to determine the appropriate parameters and structure of the subgrade.

The properties of the subgrade soil is the most important factor that influences the track modulus compared with the other track components [30]. Design of an adequate track railway should prevent subgrade progressive shear failure and excessive plastic deformation. These problems cause excessive track maintenance. In this research, the behaviour of mudrock has been examined under repeated loading and showed improvement during these cycles. However, the resilient modulus generated is only classified as medium stiffness and strength, and should be designed accordingly.

Author Contributions: S.K. conducted the experimental work and the first draft of the manuscript. S.C. and P.S. were responsible for the design of the study and the development of the manuscript. All authors have read and agreed to the published version of the manuscript.

Funding: This research was funded by The Higher Committee for Education Development in Iraq grant number D-10-1212.

Institutional Review Board Statement: Not applicable.

Informed Consent Statement: Not applicable.

Data Availability Statement: Data available in a publicly accessible repository that does not issue DOIs. This data can be found here: <https://etheses.whiterose.ac.uk/23454/> (accessed on 2 March 2022).

Acknowledgments: The first author would like to thank her co-authors and William Powrie for their guidance, valuable suggestions and support during the research.

Conflicts of Interest: The authors declare no conflict of interest.

Abbreviations

The following abbreviations are used in this manuscript:

HS1	High Speed Rail 1
SR	Stress Ratio
CDAS	Control and Data Acquisition System
PSD	Particle Size Distribution
OMC	Optimum Moisture Content

References

1. Lewis, R.; Olofsson, U. *Wheel-Rail Interface Handbook*; Elsevier: Amsterdam, The Netherlands, 2009.
2. Pombo, J.; Ambrósio, J.; Pereira, M.; Lewis, R.; Dwyer-Joyce, R.; CAriaudo, C.; Kuka, N. Development of a wear prediction tool for steel railway wheels using three alternative wear functions. *Wear* **2011**, *271*, 238–245. [CrossRef]
3. Cripps, J.; Taylor, R. The engineering properties of mudrocks. *Q. J. Eng. Geol. Hydrogeol.* **1981**, *14*, 325–346. [CrossRef]
4. Hills, C.W.W.; Denby, B. The Prediction Of Opencast Backfill Settlement. *Proc. Inst. Civ. Eng.-Geotech. Eng.* **1996**, *119*, 167–176. [CrossRef]

5. Blanchfield, R.; Anderson, W.F. Wetting collapse in opencast coalmine backfill. *Proc. Inst. Civ. Eng.-Geotech. Eng.* **2000**, *143*, 139–149. [[CrossRef](#)]
6. Nahazanan, H.; Clarke, S.; Asadi, A.; Yusoff, Z.M.; Huat, B.K. Effect of inundation on shear strength characteristics of mudstone backfill. *Eng. Geol.* **2013**, *158*, 48–56. [[CrossRef](#)]
7. Esveld, C. *Modern Railway Track*; MRT-Productions: Zaltbommel, The Netherlands, 2001.
8. Kempfert, H.; Hu, Y. Measured dynamic loading of railway underground. In Proceedings of the 11th Pan-American Conference on Soil Mechanics and Geotechnical Engineering, Foz do Iguassu, Brazil, 8–12 August 1999; pp. 843–847.
9. Bian, X.; Jiang, H.; Cheng, C.; Chen, Y.; Chen, R.; Jiang, J. Full-scale model testing on a ballastless high-speed railway under simulated train moving loads. *Soil Dyn. Earthq. Eng.* **2014**, *66*, 368–384. [[CrossRef](#)]
10. Fredlund, D.; Bergan, A.; Wong, P. Relation between resilient modulus and stress conditions for cohesive subgrade soils. In *Transportation Research Record*; Transportation Research Board: Washington, DC, USA, 1977.
11. Suiker, A.S.J.; de Borst, R. A numerical model for the cyclic deterioration of railway tracks. *Int. J. Numer. Methods Eng.* **2003**, *57*, 441–470. [[CrossRef](#)]
12. Powrie, W.; Yang, L.; Clayton, C.R. Stress changes in the ground below ballasted railway track during train passage. *Proc. Inst. Mech. Eng. Part F J. Rail Rapid Transit* **2007**, *221*, 247–262. [[CrossRef](#)]
13. Gräbe, P.; Clayton, C. Effects of principal stress rotation on permanent deformation in rail track foundations. *J. Geotech. Geoenviron. Eng.* **2009**, *135*, 555–565. [[CrossRef](#)]
14. Duong, T.V.; Cui, Y.J.; Tang, A.M.; Dupla, J.C.; Canou, J.; Calon, N.; Robinet, A. Effects of water and fines contents on the resilient modulus of the interlayer soil of railway substructure. *Acta Geotech.* **2016**, *11*, 51–59. [[CrossRef](#)]
15. Stewart, H.E. *The Prediction of Track Performance under Dynamic Traffic Loading*; University of Massachusetts Amherst: Amherst, MA, USA, 1982.
16. Lackenby, J. Triaxial Behaviour of Ballast and the Role of Confining Pressure under Cyclic Loading. Ph.D. Thesis, University of Wollongong Australia, Wollongong, Australia, 2006.
17. Suiker, A.S.J.; Selig, E.T.; Frenkel, R. Static and Cyclic Triaxial Testing of Ballast and Subballast. *J. Geotech. Geoenviron. Eng.* **2005**, *131*, 771–782. [[CrossRef](#)]
18. Czerewko, M.A.; Cripps, J.C. Assessing the durability of mudrocks using the modified jar slake index test. *Q. J. Eng. Geol. Hydrogeol.* **2001**, *34*, 153–163. [[CrossRef](#)]
19. ASTM 2699; Standard Test Method for Research Octane Number of Spark-Ignition Engine Fuel. ASTM: West Conshohocken, PA, USA, 2013.
20. Carrier, W.D., III. Goodbye, Hazen; Hello, Kozeny-Carman. *J. Geotech. Geoenviron. Eng.* **2003**, *129*, 1054–1056. [[CrossRef](#)]
21. Powrie, W. *Soil Mechanics: Concepts and Applications*; CRC Press: London, UK, 2013.
22. Franklin, J.; Chandra, R. The slake-durability test. *Int. J. Rock Mech. Min. Sci. Geomech. Abstr.* **1972**, *9*, 325–328. [[CrossRef](#)]
23. Feeley, A. *UTM-5P, Universal Testing Machine, Hardware Reference Manual*; Industrial Process Controls Limited: Boronia, Australia, 1994.
24. Promputthangkoon, P. Liquefaction of Sand-Tyre Chip Mixtures. Ph.D. Thesis, The University of Sheffield, Sheffield, UK, 2009.
25. Ahlf, R.E. M/W Costs: How they are affected by car weights and the track structure. *Railw. Track Struct.* **1975**, *71*, 34–37 + 90–92.
26. Li, D. Railway track granular layer thickness design based on subgrade performance under repeated loading. *J. Geotech. Eng.* **1994**, *120*, 939–957. [[CrossRef](#)]
27. Seed, H.B.; Chan, C.K.; Monismith, C.L. Effects of repeated loading on the strength and deformation of compacted clay. In Proceedings of the Thirty-Fourth Annual Meeting of the Highway Research Board, Washington, DC, USA, 11–14 January 1955; Volume 34.
28. Monismith, C.L.; Ogawa, N.; Freeme, C. Permanent deformation characteristics of subgrade soils due to repeated loading. In Proceedings of the 54th Annual Meeting of the Transportation Research Board, Washington, DC, USA, 13–17 January 1975.
29. Brown, S.; Lashine, A.; Hyde, A. Repeated load triaxial testing of a silty clay. *Geotechnique* **1975**, *25*, 95–114. [[CrossRef](#)]
30. Li, D.; Hyslip, J.; Sussmann, T.; Chrismer, S. *Railway Geotechnics*; CRC Press: London, UK, 2002.